CALCULATION OF MAXIMAL COLLISION FORCE IN KINEMATIC CHAINS BASED ON COLLISION FORCE IMPULSE

Mariusz Warzecha, Jerzy Michalczyk

AGH University of Science and Technology, Faculty of Mechanical Engineering and Robotics, Cracow, Poland
e-mail: mwarzech@agh.edu.pl, michalcz@agh.edu.pl

This paper presents a new method for calculating maximal collision forces in kinematic chains based on their impulses. Its main advantage is its simplicity as it is based on algebraic equations. Collisions between the feed, hammer and rotor in a hammer crusher are used as a case study to show the implementation of the proposed method. The obtained results are then compared with a reference time-domain model. The proposed method can be used by mechanical engineers in early design phases to estimate loads acting on parts during collisions as well as to search for more optimal geometrical parameters.

Keywords: collision modeling, impact force, kinematic chain, multibody

1. Introduction

The phenomenon of collision can be fundamental in the operation of a machine. This is the case when collision is used to fulfil the main function of the machine, for example in a hammer crusher, where hammers hitting the feed ensure reduction in its size. Other good examples of such machines are: pneumatic and hydraulic drills, shake-out grids, stamping or punch presses. On the contrary, collision and its effects can also be an undesirable event in the machine lifetime. Resulting from incorrect use, an accident, interaction with its surroundings, clearances between parts, or a human or control system error, it can cause substantial wear, damage and malfunctioning in machines. Collisions between the axle set of a rail-vehicle and vertical unevenness of a track (Michalczyk, 1991), a flexible-joint robot colliding with its environment (Zhang and Angeles, 2005) and collisions of ships (Bae *et al.*, 2016; Hagiwara *et al.*, 1983) are examples of such situations. Regardless of the source, assessing loads acting on parts during the collision is a challenging area for mechanical engineers, especially in the early stages of design, when the lack of part geometry limits the use of the Finite Element Method.

While considering the building blocks of a machine, subdivisions into mechanisms and kinematic chains can be made. The kinematic chains are formed by assemblies of parts connected by joints which in many practical situations are pinned joints. Such joints impose bilateral constraints on the connected parts, resulting in the limitation of the relative velocity at the connection points to 0. Due to the joints, a collision involving one of the parts of the kinematic chain results in subsequent collisions between all of its parts. To separate these two events, the initiating collision will be called an external collision, and the collisions resulting from it, internal collisions.

Khulief (2013) presented an overview of methods used for modelling collisions in multibody systems. The described methods can be divided into three approaches: generalized momentum-balance, smooth force distribution and wave propagation in flexible bodies. The generalized momentum-balance approach allows calculation of post-impact velocities and collision force impulses with a system of algebraic equations. It is, therefore, relatively easy to apply and efficient for numerical solution, but incorporates one of two assumptions for the multibody system: either

all the collisions occur sequentially (one after another) or all of them occur simultaneously. Both assumptions were applied in various studies, mostly involving multibody systems with unilateral constraints, and showed different results, which were in poor agreement with experiments (Adams, 1997; Pereira and Nikravesh, 1996; Ceanga and Hurmuzlu, 2000; Warzecha, 2018). The generalized momentum-balance methods do not allow calculation of collision force values. To obtain such values, it is necessary to allow the deformation of colliding bodies in the vicinity of the contact point and apply a compliance model. Most compliance models were directly adopted from contact mechanics (Lankarani and Nikravesh, 1994), but some incorporated concepts strictly related to the collision modelling, such as using the coefficient of restitution to model the dissipation of energy (Khulief and Shabana, 1987; Michalczyk, 2008). The local compliance models showed satisfactory agreement with experimental results for collisions of compact or stocky bodies at impact speeds up to a few metres per second (Stronge, 2018). If one of the colliding bodies is slender, which results in significant global deformation, analysis including structural vibration or wave propagation may be necessary. Such analysis requires formulation of partial differential equations for description of longitudinal and shear waves, which requires more advanced mathematical tools than in the previously described approaches. More details on this approach can be found in (Bilingham and King, 2001; Stronge, 2018).

Mechanical engineers designing systems in which impact loads have to be taken into account should find a balance between the complexity of the problem and the resulting information. The application of a generalized momentum-balance approach leads to a system of algebraic equations which are relatively simple to solve and avoid advanced mathematics, but give only information about the post-impact velocities of the bodies and the collision force impulses. The values of collision forces, which are more useful from an engineering point of view, for example to preselect needed bearings, require implementation of a compliance model and solution of a system of ordinary differential equations. Such a problem can be a challenge for an average mechanical engineer.

This article proposes a solution for the described problem of balancing the complexity and resulting information in the modelling of the collision of bodies. It discusses a method which allows calculation of the maximal collision force based on its impulse with the help of introduced algebraic equations. Thus, the mechanical engineer can assess loads acting on parts of the system being designed in the early stages of the design process, when the application of other methods, such as the Finite Element Method, is not yet possible. Therefore, more accurate choices can be made, which result in time savings in the final stages of design.

In the following Section, the reasoning behind the proposed method is given. It is followed by a simple case study supplemented with a comparison of results with a more accurate model incorporating a compliant collision force model.

2. Method

Figure 1 presents a general plane motion case of a kinematic chain colliding with an external body. This collision results in n further collisions between bodies of the kinematic chain, each of which can be characterized by the impulse of the collision force Π_i, $i = 1, \ldots, n$. Those impulses can be calculated based on generalized momentum-balance methods, but give limited information to the mechanical engineer.

To calculate the maximal values of collision forces from known collision force impulses, the following assumptions have been made:

- all collisions occur simultaneously, which is a justified assumption if the compliance of the external collision is greater than the compliance of internal collisions
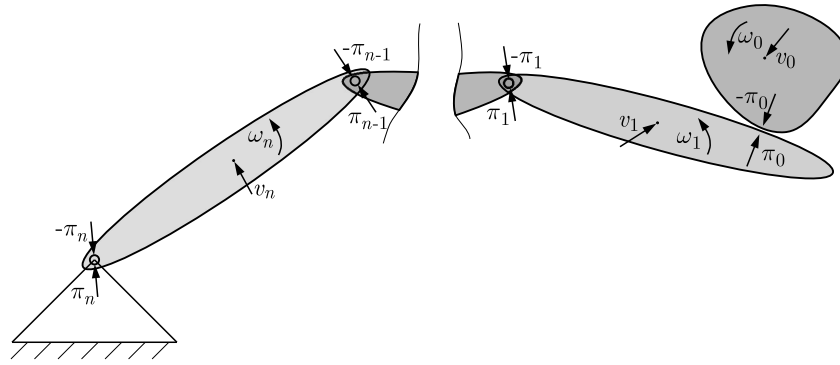- the colliding bodies are smooth (friction can be neglected)

Fig. 1. External body colliding with a kinematic chain

- the bodies are deformable near the contact area and their deformation can be described by Eq. (2.1)
- there is no energy dissipation in the compression phase of collision (but dissipation, or even destruction of one of the colliding bodies can occur in the restitution phase of collision, see (Michalczyk 2008)).

Equation (2.1) describes the local compliances of the colliding bodies by relating their deformations in the vicinity of the contact point and acting forces. As such, it can be treated as a relation describing an imaginary, non-linear spring between the colliding bodies (for $p \neq 1$)

$$P_i = k_i \xi_i^p \qquad i = 0, \ldots, n \tag{2.1}$$

where k_i is the stiffness parameter for the i-th collision, ξ_i – local deformation in the vicinity of the contact point of the colliding bodies for the i-th collision, p – exponent depending on the character of the geometrical contact of the bodies.

The collision can be divided into two phases: the compression and the restitution phase. Both phases are separated by the time point at which the relative velocity at the coincident contact point has a component normal to the common tangent plane equal to 0. This time point will be denoted as t_{max}, as the deformation and the collision force reach maximal values at this time. The value of the collision force impulse in the compression phase can, therefore, be expressed as

$$\Pi_i^* = \int_0^{t_{max}} P_i(t) \, dt \qquad i = 0, \ldots, n \tag{2.2}$$

After the introduction of two non-dimensional variables

$$\psi = \frac{t}{t_{max}} \qquad \Omega = \frac{P}{P_{i_{max}}} \tag{2.3}$$

Equation (2.2) can be written in the following form

$$\Pi_i^* = t_{max} P_{i_{max}} \Theta \tag{2.4}$$

where

$$\Theta = \int_0^1 \Omega(\psi) \, d\psi \tag{2.5}$$

can be regarded as a constant for a given value of the exponential p in Eq. (2.1). Values of Θ for the most common exponentials p are given as

$$\int_0^1 \Omega(\psi) \, d\psi = \begin{cases} 0.636 & \text{for} \quad p = 1 \\ 0.544 & \text{for} \quad p = \dfrac{3}{2} \\ 0.475 & \text{for} \quad p = 2 \end{cases} \tag{2.6}$$

Using Eq. (2.4), the relation between the collision force impulse in the compression phase and its maximal value can be written for each collision point. This gives n equations for the n unknown maximal collision forces, but they cannot be solved because of the unknown value of t_{max}. To supplement the system of equations, the kinetic energy transformed during the compression phase of collision into the strain energy of the deformed bodies is considered. Because, as assumed, there is no energy dissipation in the compression phase, the following equation can be written

$$\Delta E = E_0 - E^* = \sum_{i=0}^{n} \int_{0}^{\xi_{i_{max}}} P_i(\xi_i)\, d\xi_i \qquad (2.7)$$

where E_0 is the total kinetic energy of the colliding bodies before the collision, E^* – total kinetic energy of the colliding bodies at t_{max}.

After combining Eq. (2.1) and Eq. (2.7), the following equation is obtained

$$\Delta E = \sum_{i=0}^{n} \frac{1}{1+p} k_i^{-\frac{1}{p}} P_{i_{max}}^{\frac{p+1}{p}} \qquad (2.8)$$

Equation (2.8) allows solution of the given problem. As a result, Eqs. (2.9) are given

$$P_{i_{max}} = \frac{\Pi_i^*}{t_{max}\Theta} \qquad t_{max} = \left[\frac{1}{\Delta E} \left(\frac{1}{1+p} \Theta^{-\frac{p+1}{p}} \sum_{i=1}^{n} k_i^{-\frac{1}{p}} \Pi_i^{*\frac{p+1}{p}} \right) \right]^{\frac{p}{p+1}} \qquad (2.9)$$

Equations (2.9) allow calculation of values of the maximal collision forces based on their impulses.

3. Case study

To demonstrate an example of the implementation of the proposed method, a collision between the feed and hammer in a hammer crasher has been chosen. The goal of calculation was to establish the maximal collision force acting on the bearing of the hammer. A schematic picture of the analysed case is shown in Fig. 2. The initiating (external) collision of the feed with the hammer causes several subsequent collisions: the collision between the hammer and the rotor, the rotor and the frame, the frame and the base. For clarity of the presented example, the proposed method was applied to the first two of the listed collisions. The section has been divided into three sub-sections: calculation of collision force impulses, time-domain model and results. The first sub-section outlines the calculation of the collision force impulses in the compression phase, which are necessary to apply the proposed method. This calculation was based on the generalized momentum-balance method. The second sub-section proposes the time-domain model, which was created for reference purposes. The last sub-section provides a comparison of the maximal collision force values obtained from the proposed method and the time-domain model.

3.1. Calculation of collision force impulses

Calculation of the collision force impulses is necessary to apply the method proposed in Section 2. As such, it can be seen as a preliminary step for application of this method. The calculation was based on the generalized momentum-balance method and utilizes the fact that relative velocity of colliding bodies vanishes at the end of the compression phase. Such an approach is know from literature, i.e. Michalczyk (1991).

Two collisions occurring simultaneously at points O_0 and O_1 were analysed. The coordinate systems and the geometrical parameters used in the calculation are shown in Fig. 3.
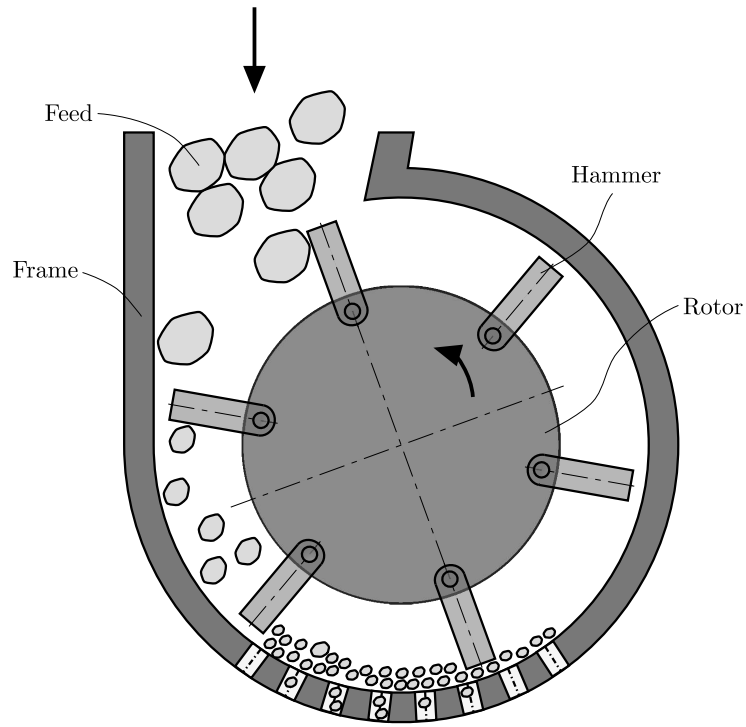
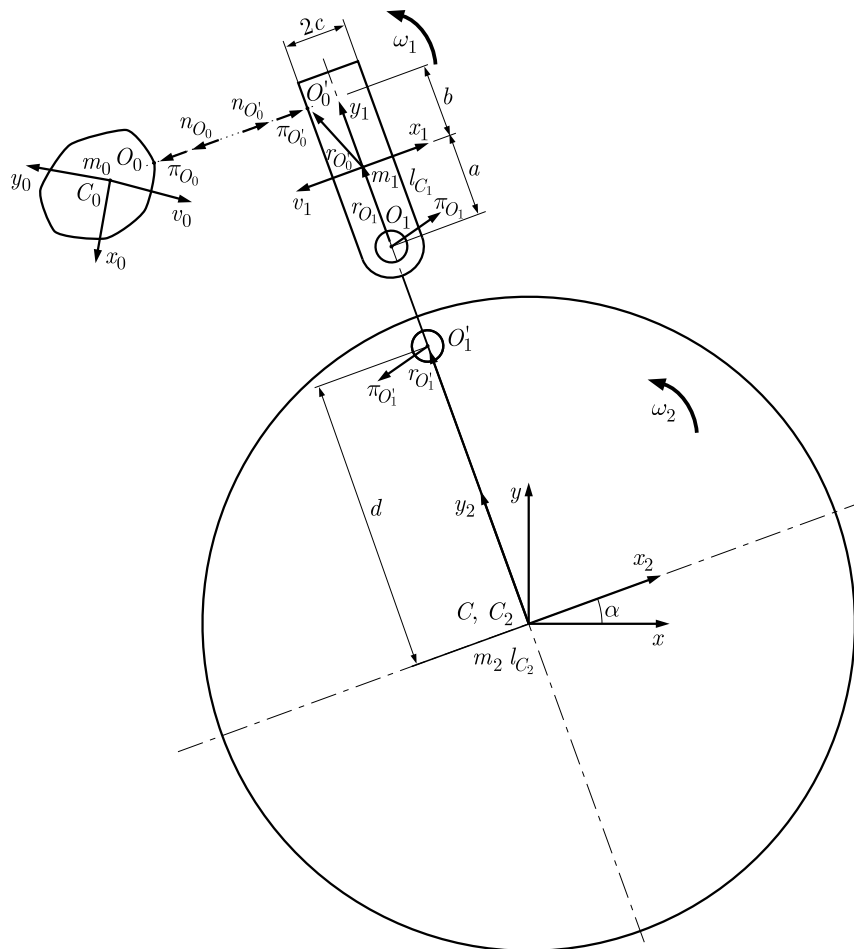Fig. 2. A schematic drawing of the analysed hammer crusher

Fig. 3. Analysed hammer crusher – applied coordinates systems, geometrical parameters and kinematic quantities

To write the equations needed for the calculation of the force impulses in the compression phase of the collision one must recognize the fact that the relative velocity of colliding bodies after its completion is equal to 0. It is, in general, a vector equation and can be written at each point in which collision occurs. In the analysed case, it is assumed that the rotor is rotating around a fixed axis, the hammer is in planar motion and the feed moves before the collision as a free body in general motion. Therefore, the analysed collisions are, in general, eccentric for all bodies. Because it is possible, as proposed in (Michalczyk, 2008), to reduce the mass of the eccentrically colliding body to the collision point and treat the collision for this body as central, such a mass is calculated for the feed and denoted as m_0^r. This was possible only for the feed as the mentioned method does not allow any additional constraints to be imposed on the body. Detailed equations were given only for the point O_0, as for the point O_1 they can be written analogously.

Equation (3.1) relates the velocities of points O_0 and O_0' along the direction normal to the common tangent plane after completion of the compression phase. As mentioned before, the relative velocity of the colliding bodies at such points is equal to 0, therefore, the values of these velocities are equal to

$$\mathbf{n}_{O_0} \cdot (\mathbf{v}_{O_0} + \mathbf{\Delta v}^*_{O_0}) = \mathbf{n}_{O_0'} \cdot (\mathbf{v}_{O_0'} + \mathbf{\Delta v}^*_{O_0'}) \tag{3.1}$$

where $\mathbf{n}_{O_0}$, $\mathbf{n}_{O_0'}$ are unit vectors normal to the common tangent plane, respectively, at the points O_0 and O_0'; $\mathbf{v}_{O_0}$, $\mathbf{v}_{O_0'}$ – velocities of the points O_0 and O_0' before collision; $\mathbf{\Delta v}^*_{O_0}$, $\mathbf{\Delta v}^*_{O_0'}$ – changes of velocity of the points O_0 and O_0' at the end of the compression phase.

The superscript $(\cdot)^*$ is used to denote the values after completion of the compression phase. Taking into account the planar motion of the hammer, Eq. (3.1) is extended to the following form

$$\mathbf{n}_{O_0} \cdot (\mathbf{v}_{O_0} + \mathbf{\Delta v}^*_{O_0}) = \mathbf{n}_{O_0'} \cdot (\mathbf{v}_1 + \boldsymbol{\omega}_1 \times \mathbf{r}_{O_0'} + \mathbf{\Delta v}^*_1 + \mathbf{\Delta \omega}^*_1 \times \mathbf{r}_{O_0'}) \tag{3.2}$$

where $\mathbf{n}_{O_0}$, $\mathbf{n}_{O_0'}$ are unit vectors normal to the common tangent plane, respectively, at the points O_0 and O_0'; $\mathbf{v}_{O_0}$ – velocity of the point O_0 before collision; $\mathbf{\Delta v}^*_{O_0}$ – change of the velocity of the point O_0 at the end of the compression phase; $\mathbf{v}_1$, $\boldsymbol{\omega}_1$ – respectively, the linear velocity of the mass centre and the angular velocity of the hammer; $\mathbf{\Delta v}^*_1$, $\mathbf{\Delta \omega}^*_1$ – respectively, changes of the linear velocity of the mass centre and the angular velocity of the hammer at the end of the compression phase.

In the next step, the velocity changes and the force impulses are related as follows:
— change of the velocity of the point O_0 at the end of the compression phase $\mathbf{\Delta v}^*_{O_0}$

$$\mathbf{\Delta v}^*_{O_0} = \frac{\mathbf{\Pi}^*_{O_0}}{m_0^r} = -\frac{\mathbf{\Pi}^*_{O_0'}}{m_0^r} \tag{3.3}$$

where $\mathbf{\Pi}^*_{O_0}$, $\mathbf{\Pi}^*_{O_0'}$ are collision force impulses, respectively, at the points O_0 and O_0' at the end of the compression phase; $m_0^{(\mathbf{r})}$ – the reduced mass of the feed,
— change of the linear velocity of the mass centre at the end of the compression phase $\mathbf{\Delta v}^*_1$

$$\mathbf{\Delta v}^*_1 = \frac{\mathbf{\Pi}^*_{O_0'} + \mathbf{\Pi}^*_{O_1}}{m_1} \tag{3.4}$$

where $\mathbf{\Pi}^*_{O_0'}$, $\mathbf{\Pi}^*_{O_1}$ – collision force impulses, respectively, at the points O_0' and O_1 at the end of the compression phase; m_1 – mass of the hammer,
— change of the angular velocity of the hammer at the end of the compression phase $\mathbf{\Delta \omega}^*_1$

$$\mathbf{\Delta \omega}^*_1 = \frac{\mathbf{r}_{O_0'} \times \mathbf{\Pi}^*_{O_0'} + \mathbf{r}_{O_1} \times \mathbf{\Pi}^*_{O_1}}{I_{C_1}} \tag{3.5}$$

where $\mathbf{\Pi}^*_{O'_0}$, $\mathbf{\Pi}^*_{O_1}$ are collision force impulses, respectively, at the points O'_0 and O_1 at the end of the compression phase; $\mathbf{r}_{O'_0}$, $\mathbf{r}_{O_1}$ – vectors describing positions of the points O'_0 and O_1 in the hammer coordinate system $C_1 x_1 y_1$; $\mathbf{I}_{C_1}$ – inertia moment of the hammer about its mass centre.

Equations (3.3), (3.4) and (3.5) are then substituted into Eq. (3.2). The described steps can be analogously taken for the collision at the point O_1. It is assumed that the angular velocity of the hammer and the rotor before collision are equal. The resulting equations, after grouping, are then written in the matrix form as follows

$$
\begin{bmatrix}
\dfrac{1}{m^r_0} + \dfrac{1}{m_1} + \dfrac{b^2}{I_{C_1}} & \dfrac{1}{m_1} - \dfrac{ab}{I_{C_1}} & 0 \\[2mm]
\dfrac{1}{m_1} - \dfrac{ab}{I_{C_1}} & \dfrac{1}{m_1} + \dfrac{d^2}{I_{C_2}} + \dfrac{a^2}{I_{C_1}} & 0 \\[2mm]
0 & 0 & \dfrac{1}{m_1}
\end{bmatrix}
\begin{bmatrix}
\Pi^{*x}_{O'_0} \\[1mm]
\Pi^{*x}_{O_1} \\[1mm]
\Pi^{*y}_{O_1}
\end{bmatrix}
=
\begin{bmatrix}
v^x_{O_0} + (a+b+d)\omega_2 \\[1mm]
0 \\[1mm]
0
\end{bmatrix}
\tag{3.6}
$$

Equation (3.6) was then solved for the unknown values of the impulses

$$
\begin{bmatrix}
\Pi^{*x}_{O'_0} \\[1mm]
\Pi^{*y}_{O'_0} \\[1mm]
\Pi^{*x}_{O_1} \\[1mm]
\Pi^{*y}_{O_1}
\end{bmatrix}
=
\begin{bmatrix}
\dfrac{m^r_0(I_{C_1}I_{C_2} + I_{C_1}d^2 m_1 + I_{C_2}a^2 m_1)(v^x_{O_0} + (a+b+d)\omega_w)}{I_{C_1}(I_{C_2} + d^2 m_1 + d^2 m^z_n r) + I_{C_2}(a^2 m_1 + m^r_0(a+b)^2) + b^2 d^2 m_1 m^r_0} \\[3mm]
0 \\[2mm]
\dfrac{-I_{C_2}(I_{C_1} - abm_1)(v^x_{O_0} + (a+b+d)\omega_w)}{I_{C_1}(I_{C_2} + d^2 m_1 + d^2 m^r_0) + I_{C_2}(a^2 m_1 + m^r_0(a+b)^2) + b^2 d^2 m_1 m^r_0} \\[3mm]
0
\end{bmatrix}
\tag{3.7}
$$

3.2. Time-domain model

As a reference and a cross-check for potential mistakes, the time-domain model of the analysed case was created. This model is valid only for a short period of time in which the collision occurs. Therefore, all forces, except for the collision ones, can be neglected as they have significantly lower values. Since the time-domain model should describe the system during both phases of collision, it was necessary to include the dissipation of energy, which was assumed to occur in the restitution phase. In view of that fact, the model of collision force given by Eq. (3.8), proposed by Michalczyk (2008), was chosen. It is convenient in use, because it allows the energy loss to be described by the coefficient of restitution

$$
P = k\xi^p \left\{ 1 - \frac{1 - R^2}{2}[1 - \operatorname{sgn}(\dot{\xi})] \right\}
\tag{3.8}
$$

To describe motion of the rotor, hammer and feed, the following coordinates have been introduced: x_0 – the position of the feed treated as a particle (see Section 3.1), x_1, y_1 – position of the mass centre of the hammer, φ_1, φ_2 – angles describing rotation of the hammer about its mass centre and of the rotor, respectively.

Using the introduced coordinates and geometrical parameters shown in Fig. 3, the following equations of motion for the analysed system are written

$$I_{C_2}\ddot{\varphi}_2 = -k_1(x_1 + \varphi_1 a + \varphi_2 d)^p \Big\{ 1 - \frac{1 - R_1^2}{2}[1 - \operatorname{sgn}(\dot{x}_1 + \dot{\varphi}_1 a + \dot{\varphi}_2 d)] \Big\} \Gamma_1 d$$

$$m_1\ddot{x}_1 = k_0(x_0 - x_1 + \varphi_1 b)^p \Big\{ 1 - \frac{1 - R_0^2}{2}[1 - \operatorname{sgn}(\dot{x}_0 - \dot{x}_1 + \dot{\varphi}_1 b)] \Big\} \Gamma_0$$

$$\quad - k_1(x_1 + \varphi_1 a + \varphi_2 d)^p \Big\{ 1 - \frac{1 - R_1^2}{2}[1 - \operatorname{sgn}(\dot{x}_1 + \dot{\varphi}_1 a + \dot{\varphi}_2 d)] \Big\} \Gamma_1$$

$$m_1\ddot{y}_1 = 0 \tag{3.9}$$

$$I_{C_1}\ddot{\varphi}_1 = -k_1(x_1 + \varphi_1 a + \varphi_2 d)^p \Big\{ 1 - \frac{1 - R_1^2}{2}[1 - \operatorname{sgn}(\dot{x}_1 + \dot{\varphi}_1 a + \dot{\varphi}_1 d)] \Big\} \Gamma_1 a$$

$$\quad - k_0(x_0 - x_1 + \varphi_1 b)^p \Big\{ 1 - \frac{1 - R_0^2}{2}[1 - \operatorname{sgn}(\dot{x}_0 - \dot{x}_1 + \dot{\varphi}_1 b)] \Big\} \Gamma_0 b$$

$$m_0^r\ddot{x}_0 = -k_0(x_0 - x_1 + \varphi_1 b)^p \Big\{ 1 - \frac{1 - R_0^2}{2}[1 - \operatorname{sgn}(\dot{x}_0 - \dot{x}_1 + \dot{\varphi}_1 b)] \Big\} \Gamma_0$$

where

$$\Gamma_1 = \begin{cases} 1 & \text{for} \quad x_1 - \varphi_1 a + \varphi_2 d > 0 \\ -1 & \text{for} \quad x_1 - \varphi_1 a + \varphi_2 d \leqslant 0 \end{cases}$$

$$\Gamma_0 = \begin{cases} 1 & \text{for} \quad x_0 - x_1 - \varphi_1 b > 0 \\ 0 & \text{for} \quad x_0 - x_1 - \varphi_1 b \leqslant 0 \end{cases} \tag{3.10}$$

Equations (3.9) constitute a system of differential non-linear equations. It was solved numerically with the help of a script implemented in Python. The following libraries were used: numpy, scipy and matplotlib.

3.3. Results

As mentioned earlier, the method proposed in Section 2 is designated for mechanical engineers as a support tool to assess loads acting on parts during collision. In order to show how it may be applied, a simple case study has been introduced. The intention was also to show a comparison of the obtained results with the time-domain model based on the literature (Lankarani and Nikravesh, 1994; Michalczyk, 2008).

To calculate numerical values of the maximal collision forces, it was necessary to obtain the values of parameters describing properties and initial conditions of the rotor, hammer and feed. The main purpose was to show the application of the proposed method and a comparison of its results with those found from the time-domain model. Therefore, the absolute values of the parameters were not of the main importance and did not represent any particular hammer crusher, but they were estimated based on known solutions. The masses and the moments of inertia were calculated based on the assumed dimensions and densities for steel (rotor, hammer) and for coal (feed). The stiffness coefficients were estimated based on the Young modulus of the mentioned materials and supposed geometry in the vicinity of the collision points. The exponential p was taken to be equal to 1.5 and the coefficients of restitution $R_0 = 0.3$ and $R_1 = 0.6$. The most important parameters are given in Table 1.

As is apparent from Table 1, several cases were investigated. Such an approach shows the ability to use the proposed method to search for more optimal parameter values at the beginning phase of design, although in this paper it was carried out rather to give more values to compare than to perform such a search as the number of analysed variants was definitely too small.

In general, the values of the maximal collision force obtained from the equations of the proposed method and the time-domain model showed reasonably small differences. As evident from Table 2 in which the obtained results were listed, the values of the maximal collision forces for the external (initiating) collision were practically equal.

Table 1. The values of parameters used in the numerical calculations

Parameter (see Fig. 3)	Value
b	150, 130, 110 mm (3 cases analysed)
a	120 mm
c	75 mm
d	500 mm
m_1	41 kg
m_2	2630 kg
I_{C_1}	0.6235 kg·m^2
I_{C_2}	757.44 kg·m^2
m_0^r	5, 10, 15 kg (3 cases analysed)
$\omega_2 = \omega_1$	62.83 s^{-1}
v_1	38.96 m/s
$\mathbf{n}_{O_0} \cdot \mathbf{v}_{O_0}$	0 m/s
R_0	0.3
R_1	0.6
p	1.5
E_{steel}	$2.05 \cdot 10^5$ MPa
E_{coal}	$3 \cdot 10^3$ MPa

Table 2. Values of the maximal collision forces obtained from the proposed method (P) and the time-domain model (F), superscript: 0 for external collision, 1 for collision between the hammer and the rotor, the values are given in kN

m_0^r	$b = 110$ mm		$b = 130$ mm		$b = 150$ mm	
5 kg	$P_{max}^0 = 750$	$F_{max}^0 = 751.6$	$P_{max}^0 = 759$	$F_{max}^0 = 758.8$	$P_{max}^0 = 767$	$F_{max}^0 = 764$
	$P_{max}^1 = 50.5$	$F_{max}^1 = 55.6$	$P_{max}^1 = 10$	$F_{max}^1 = 7.4$	$P_{max}^1 = 71.9$	$F_{max}^1 = 73$
10 kg	$P_{max}^0 = 1032$	$F_{max}^0 = 1030$	$P_{max}^0 = 1029$	$F_{max}^0 = 1033$	$P_{max}^0 = 1026$	$F_{max}^0 = 1028$
	$P_{max}^1 = 69.5$	$F_{max}^1 = 85.5$	$P_{max}^1 = 13.6$	$F_{max}^1 = 12$	$P_{max}^1 = 96$	$F_{max}^1 = 114$
15 kg	$P_{max}^0 = 1210$	$F_{max}^0 = 1207$	$P_{max}^0 = 1195$	$F_{max}^0 = 1205$	$P_{max}^0 = 1180$	$F_{max}^0 = 1183$
	$P_{max}^1 = 81.5$	$F_{max}^1 = 108.7$	$P_{max}^1 = 15.7$	$F_{max}^1 = 15.7$	$P_{max}^1 = 110$	$F_{max}^1 = 159$

The agreement of the presented results for the collision between the hammer and the rotor was noticeably worse than for the external collision. There was no consistency in the difference between them either. In some cases, the proposed method gave greater values of the maximal collision forces, whereas in others they were smaller. It is reasonable to suppose that such an outcome is related to the assumption of all collisions occurring simultaneously. This is a simplification which is made in the analysis of collisions with the use of generalized momentum-balance methods. Figure 4 shows an evolution of the collision force in time for collision between the feed and hammer, as well as for collision between the hammer and rotor. It can be seen during analysis of this figure that both collisions were overlapping, but they were not perfectly simultaneous. There was a shift between them, which is intuitively understandable.

Despite the observed differences, the proposed method gives reasonable results, especially when taking into account its simplicity and the possibility to use it in early design stages for the assessment of loads occurring during the collision. Therefore, it should be a useful tool for mechanical engineers.
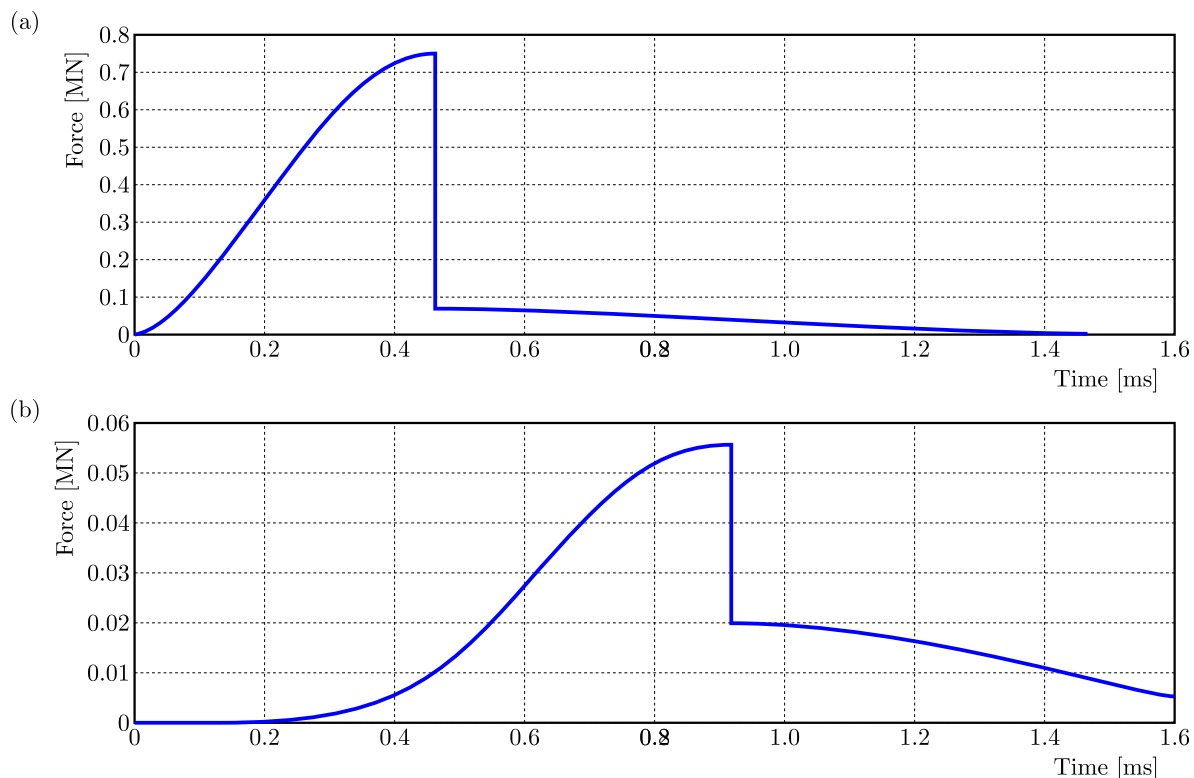
(a)

(b)

Fig. 4. Exemplary values of the collision forces in time for $b = 110$ mm, $m_0^r = 5$ kg; (a) collision force between feed and hammer, (b) collision force between hammer and rotor

4. Conclusions

This study proposes a method of calculating the maximal collision forces in kinematic chains from their impulses. It broadens the set of analytical tools available for the analysis of multi-impact problems in multibody systems with constraints, which still pose many difficulties, especially for mechanical engineers facing problems with the analysis of such phenomena in the machines designed by them. The main advantage of the proposed method is its simplicity as all needed calculations are based on algebraic equations, which may be easily implemented in commonly available software, such as a spreadsheet. The proposed method can be used in early stages of design, when 3D geometry is not yet available. It also provides the ability to analyse the influence of machine geometrical parameters on the values of the maximal collision forces. Thus, it might be used to search for more optimal values of such parameters.

The presented case study utilizes the proposed method for calculation of the maximal collision forces occurring during collision of the feed, hammer and rotor in a hammer crusher. Its main purpose was to show how the method could be applied, but the obtained results also served for comparison with outputs from the time-domain model. It was shown that the proposed method gave reasonable results. It should, however, be stated that neither method takes into account structural deformations of the colliding bodies in the global sense. The time-domain model allows only for deformation in the vicinity of the point at which the contact between colliding bodies started.

It is a known fact that structural deformations of colliding bodies can be neglected if the colliding bodies are compact. Therefore, further investigations are needed to assess when such a simplification is justified for the proposed method. It would also be beneficial to establish simple and practical rules, which could be used to decide if the results of the proposed method give acceptable levels of error. Future work is also planned to incorporate probabilistic aspects of the

collision. As it is nearly impossible to exactly predict all collision parameters (such as geometry near the contact point, material parameters, etc.), the making use of the probabilistic approach offers a promising direction for further development. It will also be interesting to compare the results of the proposed method with those obtained from the Finite Element Method, which will be the next stage of the planned research.

References

1. ADAMS G.G., 1997, Imperfectly constrained planer impacts – a coefficient-of-restitution model, *International Journal of Impact Engineering*, **19**, 693-701

2. BAE D.-M., PRABOWO A.R., CAO B., ZAKKI A.F., HARYADI G.D., 2016, Study on collision between two ships using selected parameters in collision simulation, *Journal of Marine Science and Application*, **15**, 63-72

3. BILINGHAM J., KING A.C., 2001, *Wave Motion*, Cambridge University Press

4. CEANGA V., HURMUZLU Y., 2000, A new look at an old problem: Newton's cradle, *Journal of Applied Mechanics*, **68**, 575-583

5. HAGIWARA K., TAKANABE H., KAWANO H., 1983, A proposed method of predicting ship collision damage, *International Journal of Impact Engineering*, **1**, 257-279

6. KHULIEF Y.A., 2013, Modeling of impact in multibody systems: an overview, *Journal of Computational and Nonlinear Dynamics*, **8**, 021012-1-15

7. KHULIEF Y.A., SHABANA A.A., 1987, A continuous force model for the impact analysis of flexible multibody systems, *Mechanism and Machine Theory*, **22**, 213-224

8. LANKARANI H.M., NIKRAVESH P., 1994, Continuous contact force models for impact analysis in multibody systems, *Nonlinear Dynamics*, **5**, 193-207

9. MICHALCZYK J., 1991, Analysis of collision between axle set of a rail-vehicle and vertical unevenness of a track, *Archiwum Budowy Maszyn*, **38**, 63-73

10. MICHALCZYK J., 2008, Phenomenon of force impulse restitution in collision modelling, *Journal of Theoretical and Applied Mechanics*, **46**, 897-908

11. PEREIRA M.S., NIKRAVESH P., 1996, Impact dynamics of multibody systems with frictional contact using joint coordinates and canonical equations of motion, *Nonlinear Dynamics*, **9**, 53-71

12. STRONGE W.J., 2018, *Impact Mechanics*, 2nd ed., Cambridge University Press

13. WARZECHA M., 2018, A comparative analysis of sequential and simultaneous approach in collision modeling, *Model Engineer*, **35**, 81-86

14. ZHANG D.-G., ANGELES J., 2005, Impact dynamics of flexible-joint robots, *Computers and Structures*, **83**, 25-33